Post-print of: N.A. Wójcik, P. Kupracz, R.J. Barczyński, Nonlinear electrical properties of glass-ceramics nanocomposites containing ferroelectric nanocrystallites of Bi2VO5.5, Solid State Ionics, Volume 317, 2018, Pages 7-14, https://doi.org/10.1016/j.ssi.2017.12.035.

Nonlinear electrical properties of glass-ceramics nanocomposites containing ferroelectric nanocrystallites of $Bi_2VO_{5.5}$

N. A. Wójcik [a,b,*] , P. Kupracz [a], R. J. Barczyński [a]

[a] *Faculty of Applied Physics and Mathematics, Gdańsk University of Technology, Ul. Narutowicza 11/12, 80-233 Gdańsk, Poland*
[b] *School of Engineering, Department of Built Environment and Energy Technology, Linnæus University, SE-351 95 Växjö, Sweden*

*corresponding author: natalia.wojcik@lnu.se

Abstract

Nonlinear A.C. impedance measurements were conducted in the 50BiV-50SrBAlO nanocomposite as a function of frequency, temperature and A.C. voltage. This material is ferroelectric below temperature of 730 K, and above 730 K is a good ion-conductor. For this nanocomposite a low A.C. voltage of 1 V_{rms} is enough to observe high nonlinearities. The origin of these nonlinear effects depends on the temperature and frequency. In the high temperature and low frequency region, the nonlinearities are due to interfacial processes. In the low temperatures and higher frequencies, the nonlinearities may be also correlated with ion-transport processes: hopping and blocking in glass matrix and phase boundaries. The ferroelectric properties of the $Bi_2VO_{5.5}$ nanocrystallites are also possible origin of nonlinear effects. However, their contribution into nonlinearities is weaker than from the other observed processes. It is shown that a decrease of the $Bi_2VO_{5.5}$ crystallites size from micro- to nanometers and introduction of additional structural disorder into material significantly decrease the real part of the third order electric susceptibility coefficient but does not influence the ratio of the third harmonic to the base conductivity. It is suggested that the ferroelectric nanoregions are single-domain and the nonlinearities derived from domain walls probably are not observed.

Keywords: Nonlinear conductivity; Nonlinear electric susceptibility, Glass-ceramics; Impedance spectroscopy.

1. Introduction

Dielectric properties of materials are usually investigated via linear dielectric response [1], while the higher-order susceptibilities may contain a wealth of important information [2,3]. The nonlinear effects are usually observed in high electric field [4]. Nonlinear dielectric properties were firstly measured in few liquids by Herweg in 1920/1922 [5,6] but the name Nonlinear Dielectric Effect (NDE) was originally introduced by Piekara in 1936 [7]. NDE observed in liquids is sensitive to inter-molecular interactions, intramolecular motions and inhomogenieties and may have negative or positive sign. The orientation of non-interacting or weakly interacting permanent dipoles give a negative contribution to NDE while fluctuations (inhomogeneities) give a positive contribution [8,9].

The NDE was also observed in other class of materials for instance in ferroelectrics, relaxor ferroelectrics, dipolar glasses and multiglasses [1,10-12]. However, the origin of nonlinearities observed in these systems and in liquids is different. Dielectric nonlinearity analysis of ferroelectric materials may give a deeper insight into the nature of the phase transitions.

The relation between polarization and electric field may be described as [13,14]:

$$P=\varepsilon_0(\chi_{1o}E+\chi_{2o}E^2+\chi_{3o}E^3+...) \qquad (1)$$

Where χ_{io} with $i>1$ are the higher orders susceptibility coefficients. The real part of the second order electric susceptibility coefficient (χ'_{2o}) is zero only for the centrosymmetrical systems, where the net polarization vanishes [14]. The real part of the third order electric susceptibility (χ'_{3o}) analysis may give an information about electrical parameters of state equation describing the studied system [15]. Therefore, it may allow to specify the character of the ferroelectric phase transition [16]. In the case of the

continuous ferroelectric phase transition, the critical exponents may also be determined [17, 18]. Above mentioned information was estimated only in dielectric materials with the use of D.C. or slow A.C. high electric field [1,10-12,15-18]. In these works authors have used Landau-Ginzburg-Devonshire theory of average field about thermodynamic ferroelectric phase transition [19,20].

For materials with intrinsic nonlinearities and nonstationary processes, using a nonlinear electrical method may also provide additional information about the ion transport. The magnitude and the frequency dependence of the third harmonic conductivity and third order conductivity coefficient (the real part of admittivity σ_{3h}' *(Scm^{-1})* and σ_{3o}' *(ScmV^{-2})*) may be used to provide additional clue about the apparent jump distance of ion hopping [21-25].

One of the interesting nonlinear material is $Bi_2VO_{5.5}$ ceramic [26] ferroelectric at room temperature [27-29]. Its composition may be described as $(Bi_2O_2)^{2+}(VO_{3.5}\square_{0.5})^{2-}$ where □ is an oxygen ion vacancy. $Bi_2VO_{5.5}$ exhibits three main polymorphs: a non-centrosymmetric α-phase below 730 K, a centrosymmetric β-phase above 730 K and a centrosymmetric γ-phase stable above 835 K. Both the phase transitions are of the first order (discontinuous). The high temperature γ-phase exhibits a high ionic conductivity which is attributed to the presence of oxygen ion vacancies in the V-O layer. The oxygen vacancies in α- and β-phases of $Bi_2VO_{5.5}$ also give rise to the ionic conductivity of the order of 10^{-6} to 10^{-3} $\Omega^{-1} \cdot cm^{-1}$ [30-33]. This ceramic shows high electrical nonlinearities. The ratio of the third harmonic to the base admittivity modulus (modulus of complex conductivity ($|\sigma^*| = |I\sigma' + i\sigma''|$) achieves two maxima near phase transitions temperatures and is about 0.2 under low A.C. electric field ($E_0 \leq 1.3$ kVm^{-1}) [26].

Since the $Bi_2VO_{5.5}$ ceramics exhibit nonlinear electrical properties [26], it is worth to study how the distribution in glass matrix influence on its nonlinear impedance. The

goal is to examine higher harmonics and higher orders of electrical parameters of ferroelectric glass-ceramics nanocomposites containing significant quantity of $Bi_2VO_{5.5}$ phase. The strontium-borate glass, which is a good linear dielectric with low electric permittivity [34], is selected as the glass matrix. In this work the temperature, frequency and electric field dependences of the first, second and third harmonics and orders components of conductivity, current density and electric susceptibility for $50Bi_2VO_{5.5}$-$50SrB_4O_7$ glass-ceramic nanocomposite will be analyzed and compared with nonlinear effects of the $Bi_2VO_{5.5}$ ceramic.

2. Experimental

Samples of a starting composition of $50Bi_2VO_{5.5}$-$50SrB_4O_7$ (in mol%) were prepared by conventional melt quenching technique from pre-synthesized $Bi_2VO_{5.5}$ and SrB_4O_7 substrates. The detailed description of $Bi_2VO_{5.5}$ and SrB_4O_7 substrates synthesis are described in earlier paper [35]. About 15 g of batch was placed in alumina crucibles. The glass melting was conducted at temperature of 1373 K for 30 minutes. The melts were poured onto a preheated (573 K) brass plate and pressed by another plate to obtain flat circular disks of less than 1 mm thickness and 10 - 20 mm diameter. Samples compositions were checked by Energy Dispersive X-ray Analysis (EDAX Genesis APEX 2i with Apollo x SDD Spectrometer) in 20 points on each sample. Measurement results confirmed the average amount of bismuth, vanadium, strontium and boron but aluminium were also detected. The origin of these impurities may be from alumina crucibles used. The determined average glass composition is $Bi_{58}V_7Sr_{10}B_4Al_4O_{17}$ (in wg%), where the highest discrepancies in element content are found for the lightest elements (B, Al and O) up to 2 wg%.

To obtain glass-ceramics nanocomposites, samples were heat treated up to the temperature of 813 K (above the temperature of the $Bi_2VO_{5.5}$ phase crystallization [34])

and cooled to 373 K. The heating was performed during electrical properties measurements and lasted about two days. The heat treated samples were checked by X-Ray Diffraction method with a Philips X 'Pert Pro MPD system with the CuKα radiation. The topography of the samples was investigated using a Scanning Electron Microscope (SEM), FEI Company Quanta FEG250.

For nonlinear electrical measurements, gold electrodes were evaporated onto the surface of the polished samples. Nonlinear impedance measurements were carried out in air in a frequency range from 0.1 Hz to 1 kHz with an A.C. voltage range from 0.1 to 3 V_{rms} in the temperature range from 373 to 813 K using a Novocontrol Concept 40 broadband dielectric spectrometer and a high temperature Controller Novotherm HT 1600. The measurements were carried out both while increasing and decreasing the temperature. The higher harmonic components were measured up to frequency of 1000 Hz.

In this work the impedance for harmonic components was defined as the ratio of the voltage base wave to the *n*-th harmonic current component: $Z_n^* = U_1^*/I_n^*$, where Z_n^* including the base wave generally depend on the sample voltage U_1^* base wave amplitude. From Z_n^* all other independent variables are calculated. The dependence of current density on the cosinusoidal electric field $E(t)=E_0\cos(\omega t)$ leads to the following expression:

$$j' = \sigma'_{1h} E_0 \cos(\omega t) + \sigma'_{2h} E_0 \cos(2\omega t) + \sigma'_{3h} E_0 \cos(3\omega t) + \ldots \qquad (2)$$

Where σ'_{1h} denotes base conductivity, while σ'_{2h}, σ'_{3h} etc. are higher harmonics conductivity. The admittivity for harmonic components with $n \geq 2$, is calculated from relation $\sigma^*_n = i2\pi f \varepsilon_0 \varepsilon^*_n$.

This definition of the higher harmonic complex impedance, permittivity and admittivity parameters is a simple and uniform representation for all dependent variables directly related to the measured harmonic voltages and currents.

However often another way of nonlinear polarization and current density presentation is used which is described by relation *(1)*. This convention allows calculating and analyzing higher order terms. When an A.C. cosinusoidal electric field applied, the current density being in phase with electric field, j' may be written as follows [25]:

$$j' = \sigma'_{1o} E_0 \cos(\omega t) + \sigma'_{2o} E_0^2 \cos^2(\omega t) + \sigma'_{3o} E_0^3 \cos^3(\omega t) + \cdots \quad (3)$$

Where σ_{1o}' denotes linear conductivity, while σ_{2o}', σ_{3o}' etc. are higher order conductivity coefficients. Replacing $\cos^2(\omega t)$ and $\cos^3(\omega t)$ by their Fourier transforms this becomes:

$$j' = \sigma'_{1o} E_0 \cos(\omega t) + \frac{1}{2}\sigma'_{2o} E_0^2 + \frac{1}{2}\sigma'_{2o} E_0^2 \cos(2\omega t) + \frac{3}{4}\sigma'_{3o} E_0^3 \cos(\omega t) + \frac{1}{4}\sigma'_{3o} E_0^3 \cos(3\omega t) + \cdots \quad (4)$$

According to equations *(2)* and *(4)*, the base current density j'_{1h} and the higher-harmonic current densities j'_{2h} and j'_{3h} are given by:

$$j'_{1h} = \sigma'_{1h} E_0 = \sigma'_{1o} E_0 + \frac{3}{4}\sigma'_{3o} E_0^3 + \cdots \quad (5)$$

$$j'_{2h} = \sigma'_{2h} E_0 = \frac{1}{2}\sigma'_{2o} E_0^2 + \cdots \quad (6)$$

$$j'_{3h} = \sigma'_{3h} E_0 = \frac{1}{4}\sigma'_{3o} E_0^3 + \frac{5}{16}\sigma'_5 E_0^5 + \cdots \quad (7)$$

As seen from equation *(7)*, the third harmonic current density j'_{3h} does not contain term with linear field dependence. In order to refer to literature in this work we present the analysis of both the higher harmonics and higher order coefficients.

The nonlinear electrical properties of glass-ceramics nanocomposites are compared with $Bi_2VO_{5.5}$ ceramic. The $Bi_2VO_{5.5}$ ceramic preparation, structure analysis and some part of electrical properties are presented in our earlier paper [26]. In the following part of this work samples names were simplified to 50BiV-50SrBAlO nanocomposite and BiV ceramic.

3. Results and discussion

The results of structure and topography measurements with comprehensive analysis of linear complex impedance, A.C. electric permittivity and A.C. conductivity are shown in our earlier paper [35]. XRD and EDAX investigations indicated the presence of $Bi_2VO_{5.5}$ crystalline phase in heat-treated 50BiV-50SrBAlO samples. The average crystallite size is found to be about 40 nm. It is not clearly visible in SEM micrographs if observed crystals are in direct contact to each other or whether they are separated by an insulating glassy phase. The main remark about 50BiV-50SrBAlO nanocomposite is that the $Bi_2VO_{5.5}$ phase has dominant influence on its linear electrical behaviour. In this nanocomposite two conduction process mechanisms are possible: for the low temperatures is mixed ionic–electronic and in the higher temperatures the oxygen ion hopping starts to dominate. The nanocomposite shows two distinct dispersion processes for the complex impedance and A.C. conductivity. The faster one ($f \geq 1000$ Hz) is assigned to the conduction through the $Bi_2VO_{5.5}$ nanocrystallites and is due to the high concentration of the mobile ions. The other dispersion ($10 \text{ Hz} \leq f < 1000$ Hz) may be associated with the glassy phase surrounding nanocrystallites and phase

boundaries. It is shown that in these regions the mobile ions concentration is low. There is also visible the beginning of the third process proceeding in the lowest frequency region (f <10 Hz) and in the high temperatures. This process may be related with the processes at the glass ceramic / gold interface: formation of ionic double layers and an interfacial charge transfer [35].

In this work, the second and third harmonic components were evaluated with accordance to the equation *(2)* presented in experimental part. Figure 1 shows the frequency dependence of the base conductivity, of the 2nd harmonic conductivity and of the 3rd harmonic conductivity for 50BiV-50SrBAlO nanocomposite, measured at two different temperatures (373 K and 693 K) with an A.C. voltage of 1 V_{rms} (the applied electric field amplitude E_0 = 19.6 Vcm^{-1}). In the higher temperature and low frequency range, the base and third harmonic conductivities show comparable values. At temperature of 693 K, the second harmonic conductivity values are an order of magnitude smaller than those of the third harmonic. The spectra are characterized by a D.C. plateau at low frequencies and a dispersive regime at higher frequencies. In the entire frequency range, the values of $\sigma`_{2h}$ and $\sigma`_{3h}$ are positive. Positive values and similar behavior of the third harmonic conductivity were also observed in supercooled ionic liquids but under higher fields [23, 25].

The ratio of the third harmonic to the base conductivity as a function of temperature and frequency is presented in Fig. 2. It achieves the highest values (about 0.25 at frequency of 0.1 Hz) near the ferro-paraelectric phase transition temperature characteristic for the $Bi_2VO_{5.5}$ phase (730 K) [26]. The 50BiV-50SrBAlO nanocomposite shows similar values of the ratio to the literature data for BiV ceramic [26]. However, two maxima near two phase transitions observed in ceramic are not clearly visible in nanocomposite. At higher frequencies (above 800 Hz) and lower

temperatures (below 723 K) the ratio $\sigma'_{3h}/\sigma'_{1h}$ became so small, that reliable values for σ'_{3h} could not be obtained.

In order to obtain more information about origin of the large nonlinear effects at around 1 V_{rms}, the fit results of linear impedance spectra for 50BiV-50SrBAlO nanocomposite [35] and for BiV ceramic [26] were analyzed as temperature and frequency functions. From the fitted spectra, it was deduced what fraction of the applied A.C. voltage drops over the three parts of equivalent circuit assigned to different regions observed in these two materials. Figure 3 shows the temperature dependence of fraction of applied A.C. voltage that dropped over these three regions (U_c, U_{gb}, U_{ip}) for nanocomposite ((a) 0.1 Hz and (b) 100 Hz) and ceramic ((c) 0.1 Hz and (d) 100 Hz). The U_c is the A.C. voltage fraction calculated for $Bi_2VO_{5.5}$ nanocrystallites (in nanocomposite) or crystallites (in ceramic), U_{gb} for glassy phase surrounding nanocrystallites and/or phase boundaries when the U_{ip} for the sample/gold interface, respectively. For nanocomposite it can be seen that the U_{ip} increases and the U_{gb} decreases with the increase in temperature, respectively, when the U_c rather does not depend on temperature. At low frequency region the highest fraction of applied A.C. voltage drops over the U_{ip} (Fig. 3(a)) and its value decreases with increase in frequency (Fig. 3 (b)). The opposite situation is observed for the U_{gb}, which starts to dominate at 10 Hz. The U_c value only slightly increases with frequency. The temperature behavior of A.C. voltage fractions for these regions are compared with the temperature dependence of the ratio of the third harmonic to the base conductivity to help for elucidating the origin of the strong nonlinear effects. It can be seen that only U_{ip} increases with temperature similar to nonlinearities and at low frequency region, it is clearly visible that the nonlinearities are due to interfacial processes. However, at high frequency region and temperatures lower than 703 K the values of U_{ip} and U_c are similar

and significantly lower than U_{gb}. Although, in low temperatures a few origins of nonlinear effects are possible (i.e. interfacial processes, formation of ionic double layers on phase boundaries and ferroelectric properties of nanocrystallites), an influence of the U_{ip} on third harmonic seems to be much stronger than others.

The same analysis is done for ceramic (Fig. 3(c) and (d)). However, the fit of linear impedance spectra was possible only in temperatures lower than 650 K. The conclusions for low frequency region is the same as for nanocomposite. Nevertheless, the results for higher frequencies are different. The A.C. voltage fraction for U_c shows the highest values (significantly higher than U_{ip}) at frequencies above 10 Hz and its temperature dependence is not monotonic. Therefore, we suppose that at frequencies above 10 Hz and temperatures below 650 K the processes proceeded in the ferroelectric crystallites are also possible origin of the high nonlinearities.

The electric field dependence of the base and third harmonic current densities (j'_{1h} and j'_{3h}) was further analyzed in order to calculate the higher order conductivity coefficient σ'_{3h}. Figures 4a and 4b show the j'_{1h} and j'_{3h} versus applied electric field for 50BiV-50SrBAlO nanocomposite. Both the j'_{1h} and j'_{3h} increase with electric field and temperature. The j'_{1h} increases with frequency up to specific electric field value and above its frequency dependence turns around. This specific electric field value depends on temperature and decreases with the temperature increase. It is marked by a square frame in Fig. 4a. The origin of this unexpected frequency dependence behavior is still unknown. The j'_{3h} is of about one order of magnitude lower than the j'_{1h}. It increases with the decrease in frequency for all electric field values. The field dependences of the j'_{1h} and j'_{3h} were fitted with the equations *(5)* and *(7)*, respectively. The relation *(5)* fit results show good agreement with the j'_{1h} data (Fig. 4a). It reveals that the linear and the third order terms are sufficient for describing the field dependence and higher order

terms can be neglected. From the fit, the linear conductivity σ'_{1o} and the third order conductivity coefficient σ'_{3o} values were obtained. Figure 4b shows the relation *(7)* fit results for j'_{3h} data. At higher temperatures (≥ 693 K) and lower frequencies (≤ 1 Hz) the fit results are worse. Two reasons of deviations between relation *(7)* and j'_{3h} data are possible. The first is that the values of 7th order and higher order terms are not negligible. The second more likely is that at higher temperatures and lower frequencies the interfacial effects has stronger impact on the third harmonic conductivity values. From the fits, values for the conductivity coefficients σ'_{3o} and σ'_{5o} were obtained. The values of the fifth order conductivity coefficient are negative and about two order of magnitude lower than of the third order. The results of σ'_{3o} obtained from j'_{1h} and j'_{3h} plots fitting were compared. The values were of the same order of magnitude and visible differences were found only in the dispersive regime. Similar behavior of the third order conductivity spectra derived from the j'_{1h} and j'_{3h} were observed in the supercooled ionic liquid [25]. In the further part of this work, the mean value of σ'_{3o} will be analyzed.

Figure 4c displays the electric field dependence of the j'_{1h} for different thicknesses of BiV ceramic samples (0.163 cm, 0.291 cm and 0.403 cm). The diameter of samples is the same and all samples are prepared with the same procedure described in [26]. The unexpected behavior of frequency dependence of the j'_{1h} observed for nanocomposite is not visible in ceramic. Frequency has rather small influence on the j'_{1h}. However, it is clearly visible that the j'_{1h} increases with thickness (Fig. 4c). These dependence is almost not visible for I'_{1h} (the real part of the base current) especially at higher temperatures. It may suggest that the current is limited by ionic double layer formation most likely on electrodes. The behavior of the j'_{3h} for the BiV ceramic at two different temperatures 693 K and 813 K is presented in Fig. 4d and 5, respectively. In ceramic, the j'_{3h} exhibits negative values for low electric field (A.C. voltage below 1 V_{rms}). The negative values

are clearly visible at higher temperatures (above 773 K) and frequencies (below 10 Hz). The same fitting procedure of equations *(5)* and *(7)*, was done for ceramic samples. Only j'_{1h} data show good agreement with the relation *(5)*. The fitting of j'_{3h} was insufficient. Exemplary fitting results were shown in Fig. 4c and 4d. The bad fitting results are probably caused by influence of interfacial effects. In the further part of this work, the σ'_{3o} values obtained from j'_{1h} plot will be analyzed.

Figure 6 displays the second order conductivity coefficient relative to the linear conductivity versus temperature and frequency for 50BiV-50SrBAlO nanocomposite (Fig. 6a) and for comparison for BiV ceramic (Fig. 6b). The σ'_{2o} values were calculated according to relation *(6)*. In both the materials, the ratio reaches the highest values in the temperature range below the ferro-paraelectric phase transition. Above the temperature of about 630-650 K, the $\sigma'_{2o}/\sigma'_{1o}$ ratio is small. It is known that in the case of centrosymmetrical systems the even order terms are zero and only the third and higher uneven order terms are observed [14]. The observations (Fig. 4b) are consistent with the BiV ceramic structure analysis [30,31]. Presented there research shows that this material is noncentrosymmetric in low temperature regime and centrosymmetric at higher temperatures. The same situation is visible in 50BiV-50SrBAlO nanocomposite (Fig. 4a). The $\sigma'_{2o}/\sigma'_{1o}$ ratio is significantly smaller in nanocomposite (about 0.003 at frequency of 0.1 Hz, Fig. 4a) than in ceramic (about 0.053 at frequency of 0.1 Hz, Fig. 4b).

Figure 7 shows the frequency dependence of the third order conductivity coefficients σ'_{3o} for 50BiV-50SrBAlO nanocomposite (Fig. 7a) and for BiV ceramic (Fig. 7b). The σ'_{3o} values were obtained from Fig. 4. In nanocomposite, the σ'_{3o} is positive over the entire accessible frequency (0.1 – 1000 Hz) and temperature (373 – 813 K) range. In ceramic, the situation is similar only at high temperatures. However, at

lower temperatures (below 643 K) the sign of σ'_{3o} changes from positive to negative (Fig. 8). This sign change is a general feature of ionic conductors with correlated back- and forth hopping [36].

The third order D.C. conductivity was obtained from a fit of the spectra (Fig. 7a and b) with the following empirical relation *(8)* [23]: $\sigma'_{3o} = \sigma_{3oDC}[1/(1 + af^b)]$, where a, b are coefficients and f is a frequency. The temperature dependence of σ_{3oDC} for ceramic and nanocomposite is shown in Fig. 9. The $\sigma_{3oDC}T=(T^{-1})$ shows an approximate Arrhenius behavior in temperatures around ferro-paraelectric phase transition of the $Bi_2VO_{5.5}$ phase (730 K). The activation energy of σ_{3oDC} for nanocomposite is 1.10 eV and for ceramic is 1.52 eV (below temperature of 730 K) and 0.86 eV (above 730 K). The value of activation energy of σ_{1oDC} obtained for nanocomposite is 1.19 eV [35] when for ceramic below phase transition is 0.94 eV and above is 1.27 eV [26]. For BiV ceramic, the temperature dependence of σ_{1oDC} and σ_{3oDC} differs strongly when for 50BiV-50SrBAlO nanocomposite does not. One may be noted, that the third order D.C. conductivity behavior of BiV ceramic and 50BiV-50SrBAlO nanocomposite is different therefore the processes responsible for nonlinear effects probably are not the same. The physical meaning of σ_{3oDC} activation energy values is still not clear.

The knowledge about the temperature dependence of the real part of the third order electric susceptibility coefficient (χ'_{3o}) allows to distinguish the type of ferroelectric phase transition. For the continuous transition, the χ'_{3o} during heating changes sign when for the discontinuous phase transition there is no change in sign. In ferroelectric phase, the sign of χ'_{3o} is positive in a case of both the types of transition [37].

Figure 10 displays the temperature dependence of the χ'_{3o} at frequency of 100 Hz and at A.C. voltage of 1 V_{rms} for the 50BiV-50SrBAlO nanocomposite (Fig. 10a) and BiV ceramic (Fig. 10b). It may be seen that for the BiV ceramic during heating the χ'_{3o}

stays positive and there is no change in sign around ferro-paraelectric phase transition. Similar behavior of χ'_{3o} is observed in all frequency range. This observation is in accordance with thermal analysis results of the BiV ceramic showing that both the phase transitions are discontinuous [30,31]. In the case of 50BiV-50SrBAlO nanocomposite (Fig. 10b), the magnitude of χ'_{3o} is significantly lower than in the BiV ceramic.

There are several possible origins of nonlinearities. Usually, the nonlinearity arises from interfacial processes what is visible in both the 50BiV-50SrBAlO nanocomposite and BiV ceramic at low frequency regime (< 10 Hz) and especially above temperature of 730 K (ferro-paraelectric phase transition). In the BiV ceramic in its ferroelectric phase (below the temperature of 730 K), the nonlinearities may be also due to existing domain structure characteristic for ferroelectrics. This ceramic exhibits crystallites with an average size of about 20 μm [26]. In such a case, the crystallites are multidomain separated by domain walls [38, 39]. When the linear electric susceptibility included responses only from the "pure" ferroelectric, the nonlinear electric susceptibility may contain the response from the domain walls, which were forced to move under the A.C. electric field. In nanocomposite, the $Bi_2VO_{5.5}$ nanocrystallites (with average size of about 40 nm) may be single-domain polar regions which are separated by nonpolar dielectric glass matrix. These may limit ferroelectric long-range order. Additionally in the case of single domain structure, the domain walls should not be observed what also decreases its contribution into nonlinearities.

The other possible origin of nonlinear effects is ion-transport process. The nonlinearities observed for 50BiV-50SrBAlO nanocomposite at the frequency range of 1000 - 10 Hz may be also correlated with ion hopping and blocking processes within the glassy and boundaries phases.

4. Conclusions

To conclude, 50BiV-50SrBAlO nanocomposites were prepared. Nonlinear A.C. impedance measurements were conducted as a function of frequency, temperature and A.C. voltage.

The 50BiV-50SrBAlO nanocomposite is ferroelectric below temperature of 730 K and above 730 K is a good ion-conductor. This material shows significant nonlinear electrical effects even under low electric field. The origin of these nonlinear effects depends on the processes visible in different temperature and frequency region. In the low frequency and high temperature region, the nonlinearities are due to interfacial processes. In the high frequency and low temperature range the ion hopping and blocking processes proceeded within phases with different mobile ion concentration (for instance ionic double layer formation on phase boundaries) may also give contribution into the nonlinear effects. Below the temperature of 730 K (the ferro-paraelectric phase transition of $Bi_2VO_{5.5}$), the ferroelectric properties of the nanocrystallites are also a possible origin of nonlinearities. In nanocomposite, the ferroelectric long-range order is limited and domain walls are not observed what is visible as decrease in the real part of the third order electric susceptibility. It is shown that decrease of the $Bi_2VO_{5.5}$ crystallite size from micro- to nanometers and introduction of additional structural disorder into material significantly decreases the real part of the third order electric susceptibility but does not influence the ratio of the third harmonic to the base conductivity.

Till now nonlinearities have been observed in dielectric materials only under D.C. and slow A.C high electric field. It is presented that for an ion-conducting ferroelectrics the low A.C. electric field of about $E_0=2\ kVm^{-1}$ is enough to observe high nonlinearities. Only detailed analysis of both the linear and nonlinear electrical properties give complex information about processes occurring in material.

References

[1] S. Miga, J. Dec, W. Kleemann, Nonlinear Dielectric Response of Ferroelectrics, Relaxors and Dipolar Glasses in: Dr. MickaÃ«l Lallart (Eds.) Ferroelectrics – Characterization and Modeling, Ch. 10, InTech, 2011, p. 181.

[2] X. Wei, X. Yao, Reversible dielectric nonlinearity and mechanism of electrical tunability for ferroelectric ceramics, Int. J. Mod. Phys. B, 20 (2006) 2977.

[3] X. Wei, X. Yao, Analysis on dielectric response of polar nanoregions in paraelectric phase of relaxor ferroelectrics, J. Appl. Phys., 100 (2006) 064319-1.

[4] A. Chen, Y. Zhi, DC electric-field dependence of the dielectric constant in polar dielectrics: “multi-polarization-mechanism” model, Phys. Rev. B, 69 (2004) 174109-1.

[5] J. Herweg, Die elektrischen Dipole in flüssigen Dielektricis, Z. Phys., 3 (1920) 36.

[6] J. Herweg, W. Poetsch, Die elektrischen Dipole in flüssigen Dielektricis, Z. Phys., 8 (1922) 1.

[7] A. Piekara, aturation Electrique et Point Critique dc Dissolution (Presente par Aime Cotton), C. R. Acad. Sci. Paris, 203 (1936) 1058.

[8] A. Chełkowski, Dielectric Physics; Elsevier: Amsterdam, 1980.

[9] A. Chełkowski, Dielectric Physics; PWN-Elsevier: Warsaw, 1993.

[10] W. Kleemann, S. Miga, Z. K. Xu, S. G. Lu, J. Dec, Non-linear permittivity study of the crossover from ferroelectric to relaxor and cluster glass in $BaTi_{1-x}Sn_xO_3$ ($x = 0.175–0.30$), Appl. Phys. Lett., 104 (2014) 182910.

[11] W. Kleemann, S. Miga, J. Dec, J. Zhai, Crossover from ferroelectric to relaxor and cluster glass in $BaTi_{1-x}Zr_xO_3$ ($x = 0.25–0.35$) studied by non-linear permittivity, Appl. Phys. Lett., 102 (2013) 232907.

[12] S. Miga, J. Dec, A. Molak, M. Koralewski, Temperature dependence of nonlinear susceptibilities near ferroelectric phase transition of a lead germanate single crystal, J. Appl. Phys., 99 (2006) 124107.

[13] J. Dec, W. Kleemann, S. Miga, C. Filipic, A. Levstik, R. Pirc, T. Granzow, R. Pankrath, Probing polar nanoregions in $Sr_{0.61}Ba_{0.39}Nb_2O_6$ via second-harmonic dielectric response, Phys. Rev. B, 68 (2003) 092105.

[14] C.J.F. Böttcher, Theory of Electric Polarization. Amsterdam, Oxford, New York: Elsevier, 1973.

[15] W.J. Merz, Double hysteresis loop of $BaTiO_3$ at the Curie point, Phys. Rev., 91 (1953) 513.

[16] E. Fatuzzo and W.J. Merz, Ferroelectricity. Amsterdam: North-Holland, 1967.

[17] H.E. Stanley, Introduction to phase transitions and critical phenomena. Oxford: Clarendon, 1971.

[18] J.A. Gonzalo, Set of experimental critical exponents for ferroelectric triglycine sulfate, Phys. Rev. Lett., 21 (1968) 749.

[19] V. L. Ginzburg, On the dielectric properties of ferroelectric (Seignetteelectric) crystals and barium titanate, Zh. Exp. Theor. Phys., 15 (1945) 739.

[20] A. F. Devonshire, Theory of barium titanate, Phil. Mag. Part I, 40 (1949) 1040.

[21] R.J. Barczyński, Nonlinear impedance as possible result of ion–polaron interaction in $Cu_2O–Al_2O_3–SiO_2$ glass, J. Non-Cryst. Solids, 356 (2010) 1962.

[22] S. Murugavel, B. Roling, Application of nonlinear conductivity spectroscopy to ion transport in solid electrolytes, J. Non-Cryst. Solids, 351 (2005) 2819.

[23] F. Feiten, B. Roling, Nonlinear ion transport at high electric field strengths in the ionic liquid 1-hexyl-3-methylimidazolium bis(trifluoromethanesulfonyl) imide, Solid State Ionics, 226 (2012) 59.

[24] C. Mattner, B. Roling, A. Heuer, The frequency dependence of nonlinear conductivity in non-homogeneous systems: An analytically solvable model, Solid State Ionics, 261 (2014) 28.

[25] L.N. Patro, O. Burghaus, B. Roling, Nonlinear ion transport in the supercooled ionic liquid 1-hexyl-3-methylimidazolium bis(trifluoromethylsulfonyl)imide, J. Chem. Phys., 142 (2015) 064505.

[26] N.A. Szreder, P. Kupracz, M. Prześniak-Welenc, J. Karczewski, M. Gazda, R.J. Barczyński, Nonlinear and linear impedance of bismuth vanadate ceramics and its relation to structural properties, 271 (2015) 86.

[27] A.A. Bush, Yu.N. Venevtsev, Russ. J. Inorg. Chem., 31 (1986) 769.

[28] N. Kumari, S.B. Krupanidhi, K.B.R. Varma, Dielectric, impedance and ferroelectric characteristics of c-oriented bismuth vanadate films grown by pulsed laser deposition, Mater. Sci. Eng. B, 138 (2007) 22.

[29] G. Paramesh, N. Kumari, S.B. Krupanidhi, K.B.R. Varma, Large nonlinear refraction and two photon absorption in ferroelectric Bi 2 VO 5.5 thin films, Opt. Mater., 34 (2012) 1822.

[30] F. Abraham, M.F. Debreuille- Gresse, G. Mairesse, G. Nowogrocki, Phase transitions and ionic conductivity in $Bi_4V_2O_{11}$ an oxide with a layered structure, Solid State Ionics, 28–30 (1988) 529.

[31] F. Abraham, J.C. Boivin, G. Mairesse, G. Nowogrocki, The bimevox series: A new family of high performances oxide ion conductors, Solid State Ionics, 40–41 (1990) 934.

[32] K.B.R. Varma, G.N. Subbanna, T.N. Guru Row, C.N.R. Rao, Synthesis and characterization of layered bismuth vanadates, J. Mater. Res., 5 (1990) 2718.

[33] K.V.R. Prasad, K.B.R. Varma, High-temperature X-ray structural, thermal and dielectric characteristics of ferroelectric $Bi_2VO_{5.5}$, J. Mater. Sci., 30 (1995) 6345.

[34] N. A. Szreder, P. Kupracz, M. Prześniak-Welenc, J. Karczewski, M. Gazda, K. Siuzdak, R.J. Barczyński, Electronic and ionic relaxations in strontium–borate glass and glass-ceramics containing bismuth and vanadium oxides, Solid State Ionics, 282 (2015) 37.

[35] N. A. Wójcik, M. Prześniak-Welenc, P. Kupracz, J. Karczewski, M. Gazda, R.J. Barczyński, Mixed ionic-electronic conductivity and structural properties of strontium-borate glass containing nanocrystallites of $Bi_2VO_{5.5}$. Physica Status Solidi B 1700093 (2017).

[36] H. Staesche, S. Murugavel, B. Roling, Nonlinear conductivity and permittivity spectra of ion conducting glasses, Z. Phys. Chem., 223 (2009) 1229.

[37] S. Ikeda, H. Kominami, K. Koyama, Y. Wada, Nonlinear dielectric constant and ferroelectric-to-paraelectric phase transition in copolymers of vinylidene fluoride and trifluoroethylene, J. Appl. Phys., 62 (1987) 3339.

[38] S.B. Ren, C.J. Lu, H.M. Shen, Y.N. Wang, Size-related ferroelectric-domain-structure transition in a polycrystalline $PbTiO_3$ thin film, Phys. Rev. B, 54 (1996) 14337.

[39] Hsing-I Hsiang, Fu-Fu Yen, Effect of crystallite size on the ferroelectric domain growth of ultrafine $BaTiO_3$ powders, J. Am. Ceram. Soc., 79 (1996) 1053.

Captions

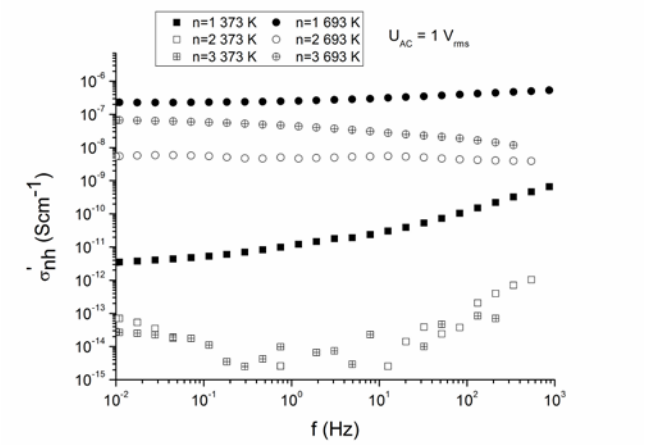

Figure 1 The base, second and third harmonic conductivity versus frequency measured at two temperatures 373 K and 693 K for 50BiV-50SrBAlO nanocomposite.

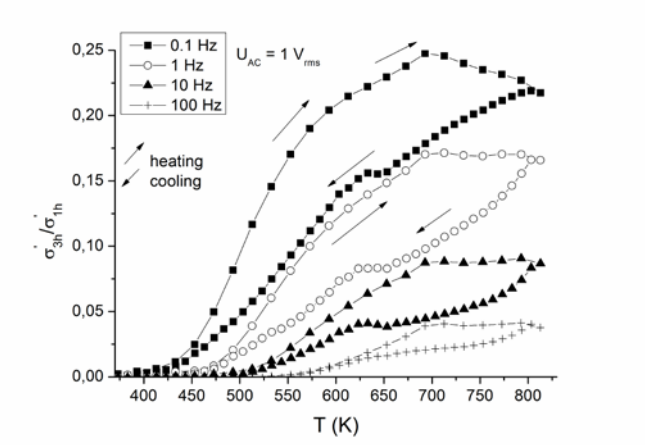

Figure 2 The ratio of the third harmonic to the base conductivity as a function of temperature and frequency for 50BiV-50SrBAlO nanocomposite.

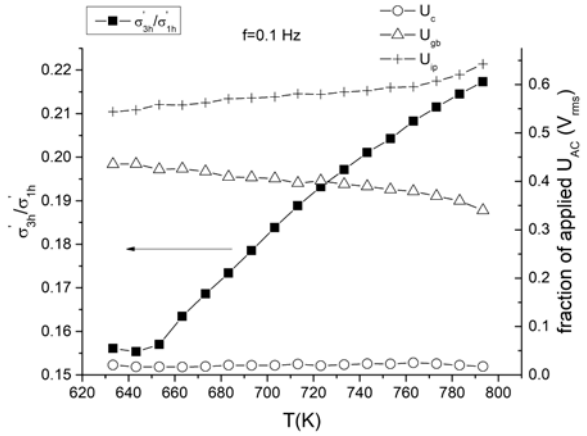

(a)

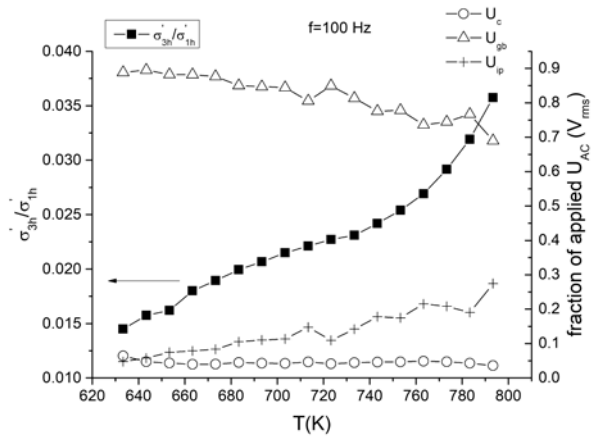

(b)

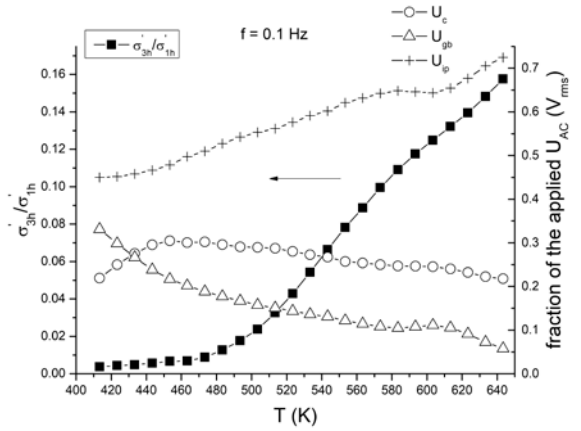

(c)

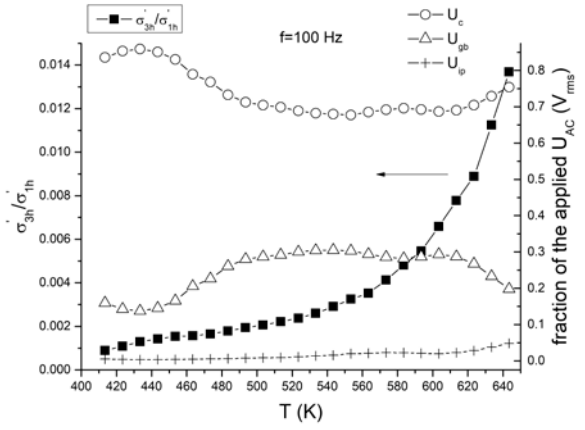

(d)

Figure 3 The temperature dependence of the fraction of applied A.C. voltage that dropped over three regions (U_c, U_{gb}, U_{ip}) and the ratio of the third harmonic to the base conductivity for 50BiV-50SrBAlO nanocomposite (**(a)** 0.1 Hz and **(b)** 100 Hz) and BiV ceramic (**(c)** 0.1 Hz and **(d)** 100 Hz). The U_c is the A.C. voltage fraction calculated for $Bi_2VO_{5.5}$ nanocrystallites (in

nanocomposite) or crystallites (in ceramic), U_{gb} for glassy phase surrounding nanocrystallites and/or phase boundaries when the U_{ip} for the sample/gold interface, respectively.

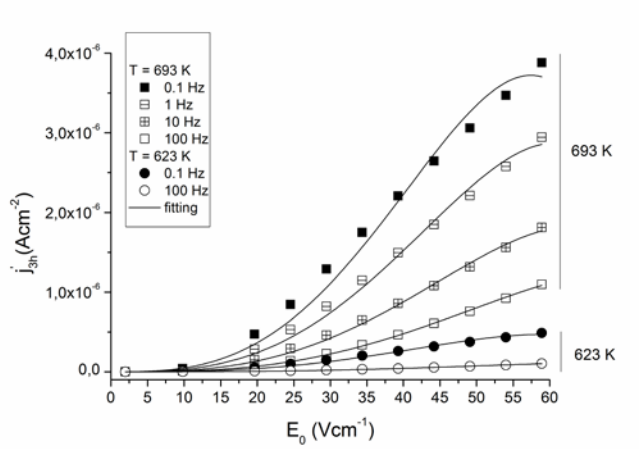

(a)

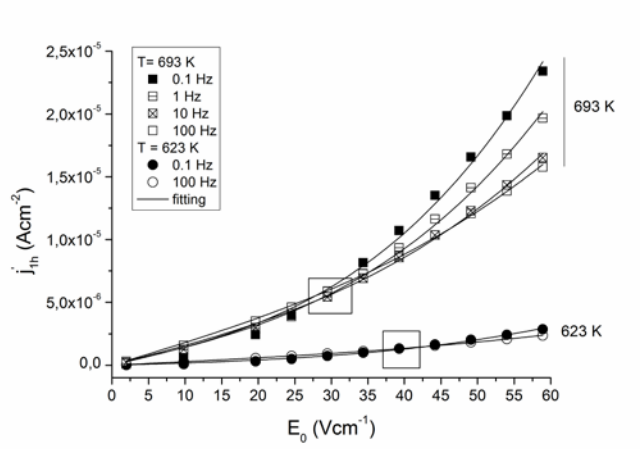

(b)

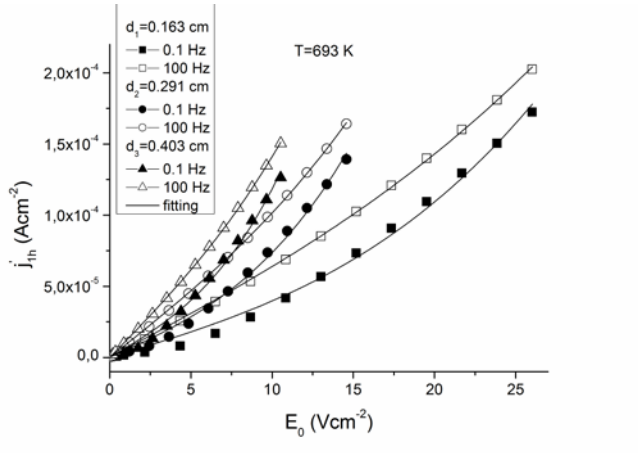

(c)

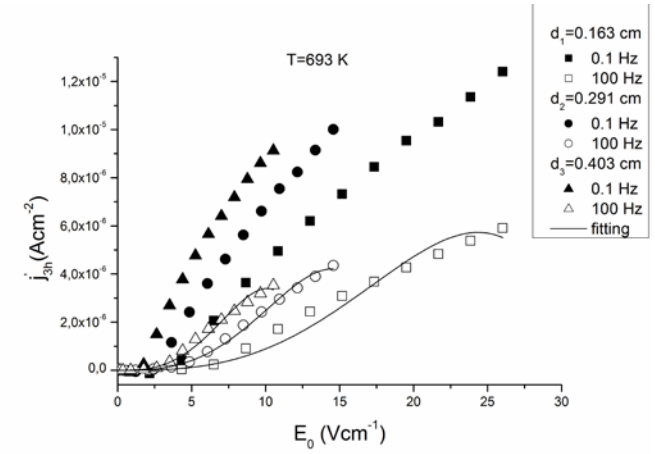

(d)

Figure 4 The real part of the first and third harmonic current density versus electric field measured at different frequencies and temperatures for **(a), (b)** 50BiV-50SrBAlO nanocomposite and **(c), (d)** for different thicknesses of BiV ceramic samples. The lines represent fits of data to $j_{1h}^{'} = \sigma_{1h}^{'} E_0 = \sigma_{1o}^{'} E_0 + \frac{3}{4}\sigma_{3o}^{'} E_0^3$ and $j_{3h}^{'} = \sigma_{3h}^{'} E_0 = \frac{1}{4}\sigma_{3o}^{'} E_0^3 + \frac{5}{16}\sigma_5^{'} E_0^5$ relations.

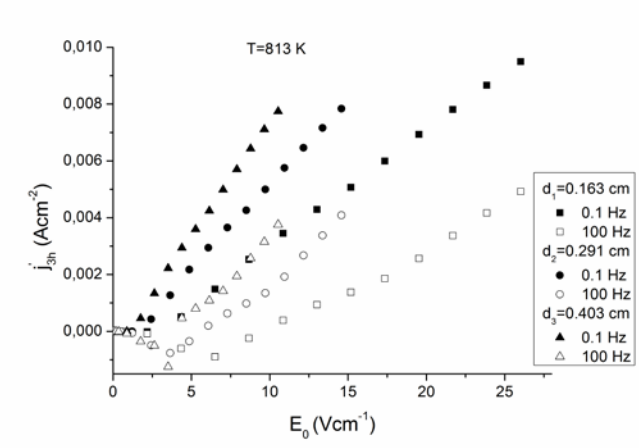

Figure 5 The electric field dependence of the real part of the third harmonic current density at temperature of 813 K for different thicknesses of BiV ceramic samples.

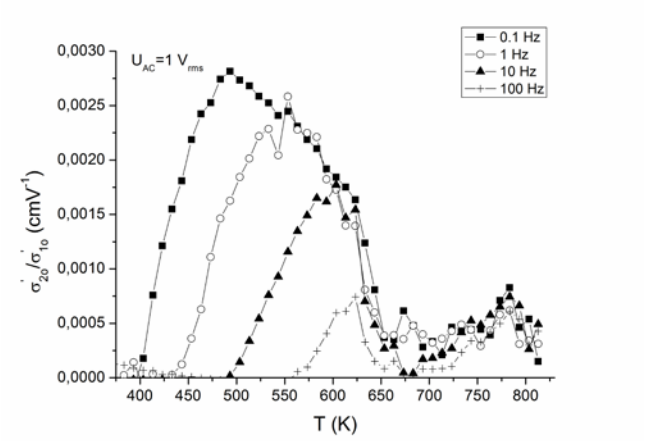

(a)

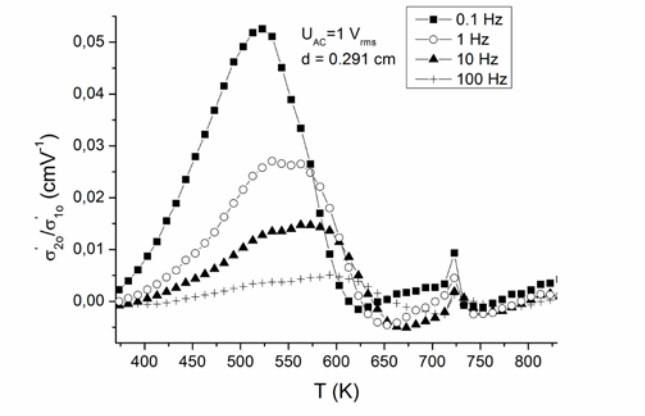

(b)

Figure 6 The ratio of the second order conductivity coefficient to the linear conductivity versus temperature and frequency for **(a)** 50BiV-50SrBAlO nanocomposite and **(b)** BiV ceramic.

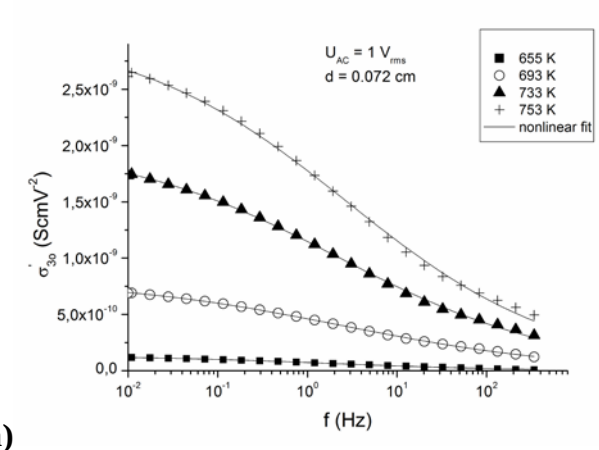

(a)

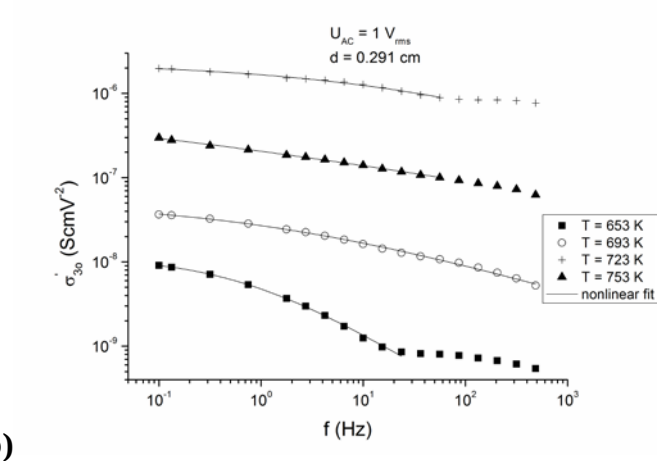

(b)

Figure 7 The third order conductivity coefficient versus frequency measured at different temperatures for **(a)** 50BiV-50SrBAlO nanocomposite and **(b)** BiV ceramic. The lines show the results of relation *(8)* fitting.

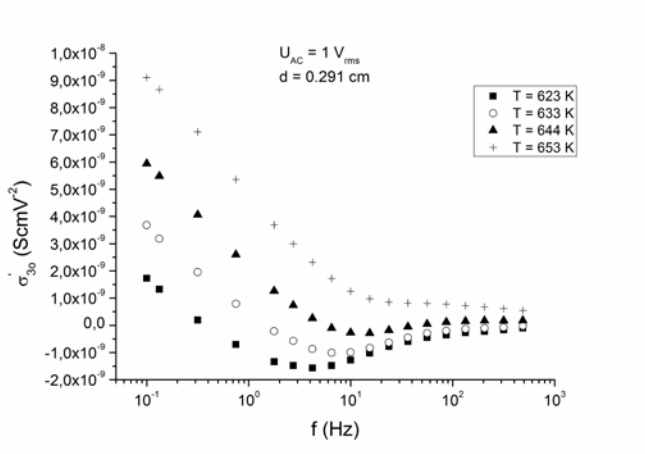

Figure 8 The frequency dependence of the third order conductivity coefficient measured at different temperatures and A.C. voltage of 1 V_{rms} for BiV ceramic.

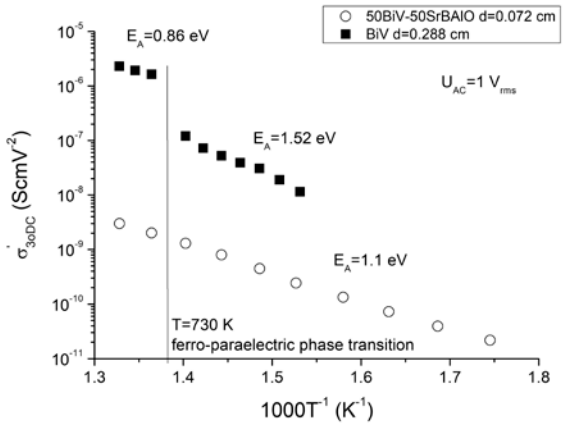

Figure 9 Arrhenius plot for the third order D.C. conductivity for 50BiV-50SrBAlO nanocomposite and BiV ceramic.

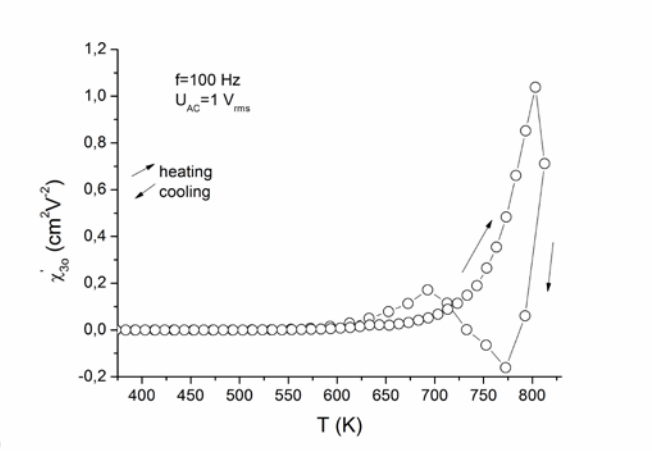

(a)

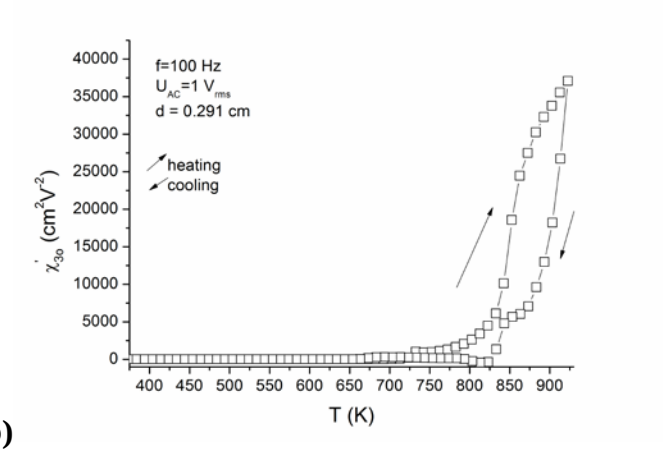

(b)

Figure 10 The temperature dependence of the real part of the third order electric susceptibility coefficient at frequency of 100 Hz and A.C. voltage of 1 V_{rms} for **(a)** 50BiV-50SrBAlO nanocomposite and **(b)** BiV ceramic.